IEEE Access
Multidisciplinary | Rapid Review | Open Access Journal

Received 16 February 2024, accepted 29 April 2024, date of publication 3 May 2024, date of current version 16 May 2024.

Digital Object Identifier 10.1109/ACCESS.2024.3396729

RESEARCH ARTICLE

Benefits of Employing Surface Electromyography Signals for Power-Assisted Control From an Agility Perspective

JAEWON BYUN[1] AND KEEHOON KIM[1,2], (Senior Member, IEEE)
[1]Department of Mechanical Engineering, Pohang University of Science and Technology (POSTECH), Pohang, Gyeongbuk 37673, Republic of Korea
[2]Institute for Convergence Research and Education in Advanced Technology, Yonsei University, Seoul 03722, Republic of Korea

Corresponding author: Keehoon Kim (khk@postech.ac.kr)

This work was supported in part by the National Research Foundation of Korea (NRF) Grant funded by Korea Government (MSIT) under Grant 2022M3C1A3081359; in part by the Technology Development Program funded by the Ministry of SMEs and Startups (MSS, South Korea) under Grant S3177366; and in part by the Institute of Information and Communications Technology Planning and Evaluation (IITP) grant funded by Korea Government (MSIT), Development of Interaction Technology to Maximize Realization of Virtual Reality Contents Using Multimodal Sensory Interface, under Grant 2021-0-00986.

This work involved human subjects or animals in its research. Approval of all ethical and experimental procedures and protocols was granted by the Institutional Review Board (IRB) at POSTECH for Human Subject Tests under Application No. PIRB-2022-E012.

ABSTRACT This paper discusses the benefits of employing surface electromyography (sEMG) signals for power-assisted control to recognize human motion intention swiftly and efficiently from an agility perspective. A majority of power-assisted control systems use interaction force and torque (F/T) sensors to recognize human motion intention. However, these sensors have limitations regarding agility as they are fundamentally indirect and delayed measurement sensors. As a direct sensor to recognize human motion intention prior to actual human body movements, this study focuses on elucidating the benefits of sEMG-based power-assisted control, which can serve as a complementary and synergetic method alongside the widely used F/T-based power-assisted control. Our experimental (n = 11) results suggest that sEMG-based power-assisted control can increase the agility of inherent body movement through correct and rapid recognition of intention. We evaluated agility with respect to muscle usage and elapsed time for task completion, considering the meaning of agility. The results are as follows: the sEMG-based method reduced 1) muscle usage by 29.45% for the trajectory following task, 2) muscle usage by 25.92% and elapsed time by 5.61% for the step response task, and 3) muscle usage by 16.68% and elapsed time by 7.14% for the maximum speed of repetitive movement task, all compared to those of inherent body movement.

INDEX TERMS Agility, exoskeleton, sEMG, motion intention recognition, physical human-robot interaction, power-assisted control, wearable robotics.

I. INTRODUCTION

Power-assisted robots provide physical assistance to individuals with insufficient muscle abilities and have been successfully used to enhance mobility and amplify power in various fields, including military [1], industry [2], and rehabilitation [3]. Physical assistance is also necessary for activities of daily living (ADLs). For example, elderly individuals or patients with limited inherent restrictions in body movement require more effortless or faster movements in ADLs. In such cases, the ability to move the body quickly with low muscle effort is called agility [4], which can be described as a light movement. Hence, to provide assistance from the agility perspective, power-assisted robots should facilitate more rapid movements with reduced muscular effort compared to the inherent body movement.

Several control strategies have been developed to operate power-assisted robots for various tasks and applications. When a task has a clear purpose or involves repetitive motion, predefined trajectories have been effectively used

The associate editor coordinating the review of this manuscript and approving it for publication was Giacinto Barresi.

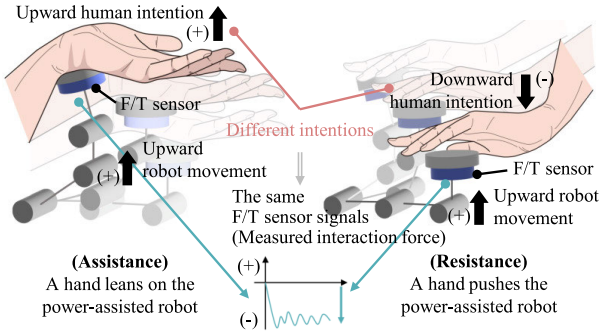

FIGURE 1. Using F/T signals can lead to the incorrect recognition of human intention, as the same signal can be measured for different intentions, such as providing assistance or resistance. Increasing agility requires a robot to push the human body toward the intended movement, causing the human body to lean on the robot. Consequently, interaction forces act in opposite directions on the robot and human body due to the action-reaction principle. This characteristic causes the interaction to be measured in the same direction, even for different intentions. Hence, it is difficult to distinguish motion intention, especially intended direction, between assistance and resistance conditions.

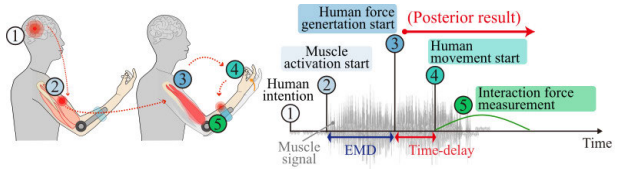

FIGURE 2. The time-delay issue of F/T signals arises because the interaction force is measured after human movement. Thus, when the F/T signal is used to recognize the human intention, the robot follows the intention belatedly, resulting in delayed assistance. Additionally, when the intention changes rapidly, it may lead to the incorrect recognition of the intention.

with promising results such as gait assistance [3]. However, predefined trajectories may lack flexibility and be unsuitable for adapting to unexpected situations arising from variations in human intention. In response, intention-based methods have been investigated in various situations. A straightforward approach is using external devices such as buttons [5] or joysticks [6]. Although the external device can clearly detect the intention, it can cause a cognitive burden because manipulating an external device is not intuitive for human motion. Additionally, it restricts the use of hands, resulting in missed opportunities to perform intricate tasks. Inertial measurement unit (IMU) is an alternative to detect motion intention by capturing movement effectively. However, they are applicable to only observable movements [7]. Alternatively, an interaction F/T sensor can detect intention during the physical interaction between the human and robot without cognitive burden. Furthermore, it can measure the interaction force with reliability and clear causality even in the absence of observable motion.

Based on these advantages, F/T-based power-assisted controls have been used successfully to reduce robot impedance and carry payloads [8], [9], [10]. However, using F/T signals to recognize human intention for agile movement has two major drawbacks: 1) the possibility of recognizing human intention incorrectly with the interaction F/T signal because the signal has the same direction for different intentions, such as assistance and resistance, as shown in Fig. 1; and 2) time-delayed recognition of intention since it is a posterior result for the human force as shown in Fig. 2. These limitations arise because the F/T sensor measures human intention indirectly. Furthermore, these limitations lead to slow and misguided assistance for agile movement. It will be discussed in Fig. 1 and 2, and Section II, in detail.

A solution to these drawbacks is achievable by employing the bio-signal as a direct signal of motion intention. Electroencephalography (EEG) is often used to detect human intention by measuring brain activity signals, but it remains still challenging [11]. Among the bio-signals, sEMG signals have been widely used to recognize motion intention as they are directly related to movement and can be measured easily from the skin surface [12], [13]. Additionally, it can be measured before human force generation, and this characteristic is referred to as the electromechanical delay (EMD) [14]. Therefore, the sEMG signal can be expected to provide a correct and rapid measurement to recognize the intention.

In a previous study [15], the limitations of the F/T-based method were explained and addressed using the sEMG signal under unknown external perturbations. In [16], a comparative study of the intention-detection strategy between F/T-based and sEMG-based controllers was conducted. Several researchers have used the sEMG-based control in power-assisted robots [12], [13], [17], [18], which focused on the sEMG signals as one of the sensor signals to decode motion intention. However, there is a lack of experimental evidence and discussion of the benefits of sEMG signals and the limitations of F/T signal, i.e., the discrepancy between F/T signal and motion intention and time-delay issues, from an agility perspective.

This study quantitatively discusses the benefits of using sEMG signals to recognize motion intention for power-assisted control from an agility perspective, mainly based on experimental results. Additionally, this study illustrates that sEMG-based control can enhance the limitations of F/T signal by enabling correct and rapid power assistance.

The remainder of this paper is structured as follows. In Section II, we review the conventional F/T-based power-assisted control method and analyze the limitations of F/T-based control for agile movements. Then, in Section III, we set up three comparison experiments to verify the benefits of employing sEMG signals in power-assisted control. The experimental results, in terms of agility, are presented in Section IV. Section V discusses the benefits of employing sEMG signals to enhance agility based on the experimental results. Finally, the conclusions are presented in Section VI.

II. PROBLEM DEFINITION

In this section, we review the power-assisted control methods that use F/T signals to recognize human intention. Additionally, we describe the limitations of F/T-based power-assisted

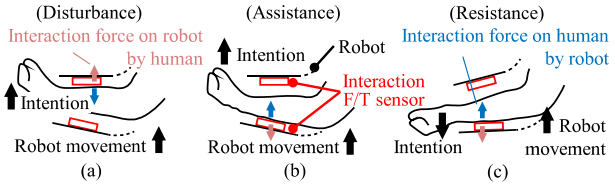

FIGURE 3. The possible interaction statuses of coupled-system between the forearm and robot for the motion intention from an agility perspective. The blue and red arrows represent the interaction forces work on the forearm and F/T sensor, respectively. (a) Human pushes the robot while feeling the robot's impedance. (b) The forearm is assisted by the robot. (c) Human resists the motion of the robot. (a), (b), and (c) correspond to areas A, B, and C in Fig. 5, respectively.

control for human intention recognition from an agility perspective.

A. PROBLEM STATEMENT

This study aims to verify the benefits of employing sEMG signals for power-assisted control to enhance the agility of body movement. The robot should recognize human motion intentions correctly and rapidly to enhance agility. This is because incorrect recognition can result in the opposite direction of the motor input, which could disturb human motion. Additionally, delayed intention recognition can cause delayed control input, and as a result, the robot may follow the human movement belatedly after the human is already in action. This delay can disturb human movements and be particularly disruptive when an individual changes intention.

To summarize, for a power-assisted robot to significantly improve agility, it is essential to ensure the following criteria:

1) Accurate and reliable interpretation of the user's motion intention.
2) Minimizing time delay in recognizing human motion intentions to ensure closer alignment between the user's actions and the robot's power assistance.
3) Assistance to the human user in conserving energy while simultaneously enhancing movement speed.

B. LIMITATIONS OF FORCE/TORQUE-BASED CONTROL METHODS ON AGILE MOVEMENT: A MATHEMATICAL ANALYSIS

While interaction F/T signals exhibit limitations in recognizing intention for agile movements, prior applications in previous studies have proven successful, offering valuable insights into the control framework. These frameworks are also applicable to employing sEMG signals as command sources instead of F/T signals. In [8], an admittance control framework was developed by incorporating the intention to deal with the unknown masses and moments of inertia of the robot. An intention-guided control was also proposed for an upper-limb power-assist exoskeleton with a force-sensing resistor and admittance control [9]. In [10], a passivity-based nonlinear admittance control method provided assistance for an unknown payload while recognizing the intention via the F/T sensor. In these studies, the F/T sensor can successfully recognize motion intention because the human interacts with

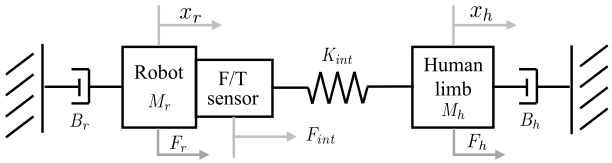

FIGURE 4. Simplified dynamic model of the coupled system between human limb and robot.

the robot based on the intended motion, resulting in alignment between the measured F/T signal and the motion intention, as shown in Fig. 3-(a) and (c). Then, they perform assistance by reducing the impedance of the robot or payload with the F/T signal.

On the other hand, when enhancing agility, the robot should push the human limb, such as Fig. 3-(b). This means that the power-assisted control should provide sufficient assistance to reduce the impedance of not only the robot but also the human body. Therefore, the intention and the interaction force cannot be in the same direction due to the action-reaction principle, as shown in Fig. 1. Additionally, there is a difference in the perspective of the time delay effect. In previous studies that utilized F/T signals, it was sufficient to provide assistance after human force generation because the focus is on the impedance of the robot or payload. However, to enhance agility compared to inherent body movement, late assistance is a critical issue since the robot should provide assistance not for the robot movement but for the body movement. Delayed assistance does not involve assisting human actions directly but rather involves the robot following the human's movements. Therefore, we need to reconsider the signal when recognizing the intention for power-assisted control to increase agility.

The delay in the F/T signal can be explained by the causal relationship of physical human-robot interaction that occurs after human movement, as explained in Fig. 2, and previous studies [19], [20]. However, to the best of the author's knowledge, no literature has discussed the discrepancy between F/T signal and motion intention. Therefore, we present descriptions that interaction F/T signal can be the same direction for the different intentions, and vice versa.

Fig. 4 shows a simplified schematic diagram describing the coupled system between the human and robot. x and F represent the position and force, respectively. Mass, damping, and gravitational force are described by M, B, and G, respectively. The subscripts $(\cdot)_h$, $(\cdot)_r$, and $(\cdot)_{int}$ represent the values for humans, robots, and interaction, respectively. The subscripts $(\cdot)_w$ and $(\cdot)_{wo}$ indicate with and without a robot, respectively.

We can represent the interaction force such as:

$$F_{int} = K_{int}(x_{h,w} - x_{r,w}) \tag{1}$$

considering the direction of the sensor. The interaction force is measured by the relative position between the human limb and the robot and the stiffness of the interface connecting the human limb and the robot, denoted as K_{int}. The

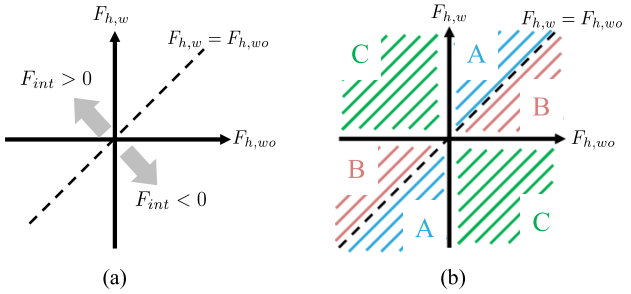

FIGURE 5. (a) Sign of the interaction torque according to the (4). (b) Conditions for each interaction status. Area-A represents disturbance, area-B represents assistance, and area-C represents resistance statuses via power-assisted robot. The measured interaction torque can be in the same direction for different situations and intentions.

Fig. 3-(a) and (b) show that the F/T signal can be in a different direction for the same intention since it can detect only the positional differences between the human limb and the robot, which is indirect to the human intention, i.e., F_{int}, not F_h.

Additionally, we can show that the F/T signal can be in the same direction for different intentions, such as Fig. 3-(b) and (c). The dynamics of the human limb without and with the assistance robot are as follows [21]:

$$M_h\ddot{x}_{h,wo} + B_h\dot{x}_{h,wo} + G_h = F_{h,wo} \tag{2}$$

$$M_h\ddot{x}_{h,w} + B_h\dot{x}_{h,w} + G_h = F_{h,w} - F_{int} \tag{3}$$

For the same movement which means $X_{h,w} = X_{h,wo}$ where $X_h = [x_h\ \dot{x}_h\ \ddot{x}_h]$, we can obtain following relationship.

$$F_{h,wo} = F_{h,w} - F_{int} \tag{4}$$

We can determine several conditions with this relationship. The blue area (A) in Fig. 5, corresponding to Fig. 3-(a), is in a state of disturbance since $F_{h,w}/F_{h,wo} > 1$, which implies that the human uses more force for the same movement, showing that the human needs to overcome the impedance of the robot and apply more human force. However, the red area (B) in Fig. 5, corresponding to Fig. 3-(b), is the assistance condition because $F_{h,w}/F_{h,wo} < 1$. This implies that humans use less force for the same movement. Conversely, the green area (C) in Fig. 5, corresponding to Fig. 3-(c), showing different directions of $F_{h,w}$ and $F_{h,wo}$, is the resistance condition. This is because the human generates a force ($F_{h,w}$) in the opposite direction to the original human force ($F_{h,wo}$) for the same movement. This implies that humans resist incorrect robot input. Likewise, using the F/T signal alone to determine intention is difficult because it can be in the same direction for different intentions.

III. EXPERIMENTAL METHODOLOGY

We set up experiments to verify the benefits of employing sEMG signals to enhance agility. To analyze the characteristics of employing each signal, four conditions, described in Fig. 7, were compared in three comparison experiments for elbow motion. This study was approved by the institutional review board (IRB) at POSTECH for human subject tests (number PIRB-2022-E012).

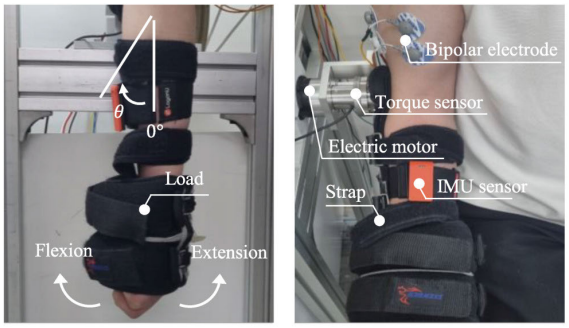

FIGURE 6. Configurations of a 1-DOF system (a) Overview of the arm and load (b) Electric motor, torque sensor, IMU sensor, and electrodes. The subject performs elbow motion while sitting, aligning the axis of the elbow and motor, and tightening the strap sufficiently.

A. HARDWARE CONFIGURATION

Experiments were conducted using a 1-DOF system for elbow motion assistance, as shown in Fig. 6. EtherCAT was selected as the communication protocol for implementing 1 kHz real-time data acquisition (DAQ) and control. An EC-iø52mm brushless motor (Maxon Motor, Switzerland) was synchronized with the other DAQ devices. The motor is equipped with a 43:1 reduction gear so that the maximal continuous torque becomes 27.52 Nm. An M2210A torque sensor (Sunrise, China) was installed to capture the interaction torque between the forearm and robot, and its signal was amplified and acquired from ClipX (Beckhoff, Germany). The DAQ interface, visual feedback and real-time data processing were implemented using Microsoft Foundation Classes(MFC). sEMG signal recordings passed through a Model 1800 AC amplifier (A-M Systems, USA) with an internal notch filter of 60 Hz, band-pass filter ranging from 10 to 500 Hz, and gain of 10,000. The sEMG signal was captured from a bipolar conductive adhesive hydrogel-type electrode (Covidien, Ireland) considering the notifications about factors that impact the sEMG signal according to SENIAM recommendation [22]. Target muscles were selected as the triceps brachii for the extension muscle and biceps brachii for the flexion muscle. A wire-based sEMG acquisition system was used to reduce the transmission time delay of the signals. An IMU sensor (March Bionics, Korea) captured the angle of the elbow joint not for the control of a robot but for validation of the results.

B. PROTOCOL

Eleven (N=11) healthy male subjects participated in the experiment. The participants were included through preliminary assessments and self-reports to ensure the following criteria: no history of musculoskeletal or neurological diseases, normal muscle strength, and normal joint range of motion. The load (5.18 kg ± 1.55 kg), which can produce approximately 50% of the maximal torque of the subject measured during MVC, was affixed on the subject's forearm. The MVC measurements were performed with the elbow positioned at 90 degrees. The presence of the load

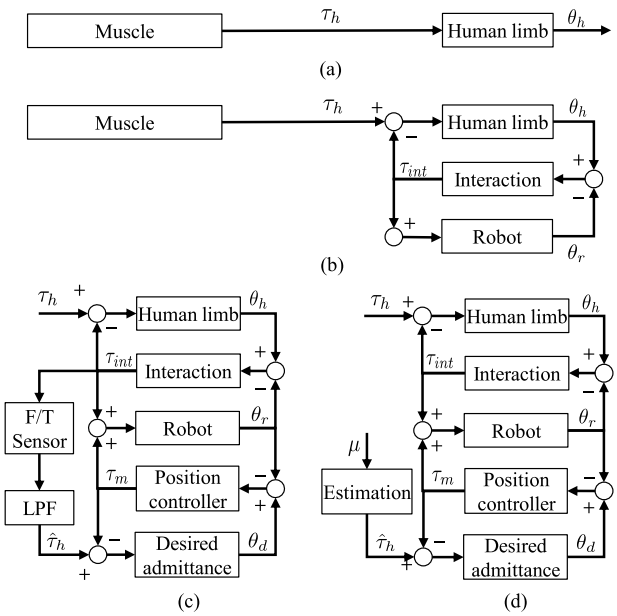

FIGURE 7. Four comparison conditions of the experiments. (a) *inherent motion (baseline)*: Subjects moved the body without a robot. (b) *no assistance*: Subjects wore the robot. No controller was applied to the robot. (c) *F/T-based*: Subjects wore the robot. The interaction F/T signal was used for intention recognition. (d) *sEMG-based*: Subjects wore the robot. The sEMG signal was used for intention recognition. (c) and (d) are passivity-based admittance control(shaping) schemes. τ and θ indicate the torque and angle, respectively. μ indicates the sEMG signal. $\hat{\tau}_h$ means estimated human joint torque.

increases the impedance of the subject's forearm, resulting in conditions requiring power assistance.

We conducted a comparative experiment for four conditions described in Fig. 7.

1) **Inherent motion (baseline)**: Subjects do not wear the robot such as Fig 7-(a).
2) **No assistance**: Subjects wear the robot. Any controller is not applied to the robot Fig 7-(b).
3) **F/T-based**: Subjects wear the robot. The passivity-based admittance control is applied to the robot using the interaction F/T signal as human intention, such as Fig 7-(c). The details of the controller are explained in Section III-C.
4) **sEMG-based**: Subjects wear the robot. The passivity-based admittance shaping control is applied to the robot using the sEMG signal to recognize the human intention, such as Fig 7-(c). The details of the controller are explained in Section III-C.

Three experiments were conducted, with subjects performing the task under each of the four conditions in a random sequence. The subjects could monitor their current position and informed that they should give their best effort during these experiments. They rested sufficiently between each trial to avoid muscle fatigue. The experiments are as follows:

1) **Experiment #1 - Following a reference trajectory**: The subjects follow the reference trajectory five times for elbow motion. The reference trajectory described in Fig. 8-(a) was introduced for visual feedback to the user to enable a fair comparison of the four conditions with the same task and to confirm the possibility of assistance in slow motion.
2) **Experiment #2 - Step response**: The subjects were asked to move the forearm as fast as possible to reach the target position, which is the step response, five times. The target position is 90° and starts at random timing.
3) **Experiment #3 - Maximum speed of repetitive movement**: The subjects were asked to repeat the elbow motion ten times between 0° and 90° as quickly as possible.

C. REAL-TIME CONTROLLER

We utilized a passivity-based admittance control method [10] in this experiment that follows system dynamics into a user-defined nominal system and enables safe interactions between the robot and human via an interconnection of passive systems. Then, we used the interaction torque signal and sEMG signal to recognize human intention as shown in Fig. 7-(c) and (d).

When using the interaction torque signal (*F/T-based*), the controller is shown in Fig. 7-(c), and it is the same with previous works [10]. We applied a low-pass filter (LPF) to deal with the noise of interaction torque signals with 5 Hz cutoff frequency, considering the bandwidth of human movement.

When using sEMG signal (*sEMG-based*), the control structure is shown in Fig. 7-(d). The control scheme can be used safely even with sEMG signals as an input, without breaking passivity as proved in [10].

The controller's gains were set to ensure sufficient assistance while minimizing any sense of discomfort due to the excessive assistance for the user through preliminary tests and feedback from the subjects. The subjects were allowed to become familiar with the system and control methods.

The sEMG signal is filtered as mean-absolute-value (MAV) in this study because it is too noisy to be used directly in the control scheme [23]. MAV (μ_{MAV}) was used, which can be calculated using the moving average of the absolute value of the raw sEMG signal (μ_{raw}) as below because it is a simple and well-used method for smoothing noisy signals.

$$\mu_{MAV}(k) = \frac{1}{W} \sum_{j=k-N+1}^{k} |\mu_{raw}(j)| \tag{5}$$

where W is the window size of the moving average, and it is $W = 100$ that is 100 ms in this study considering the effect of window size, as explained in Section V-C.

Also, we utilized the fact that the relationship between the sEMG signal and joint torque is exponential [15] to recognize human intention. In detail, the estimation model that can be used simply and effectively is as follows:

$$\hat{\tau}_{i,h} = \mu_{i,MAV}^{a} \cdot exp(b - c \cdot \mu_{i,MAV}) \tag{6}$$

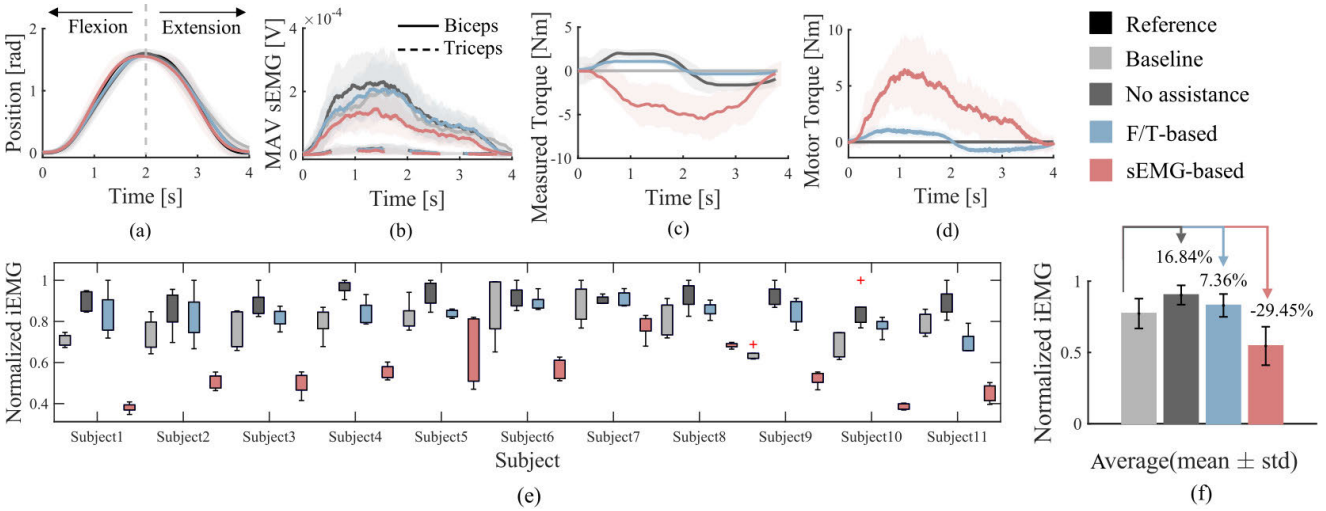

FIGURE 8. Experiment #1: Results for the following a reference trajectory experiment. (e) is a box plot for each subject's result. (f) shows the total average and standard deviation of iEMG values for each condition, with percentages representing the value compared to the *baseline*.

where $a, b,$ and c are user parameters [24] and subscript i represents flexion or extension. The parameters are estimated through the nonlinear regression with the sEMG and torque data acquired through the maximal voluntary contraction (MVC) process. This was conducted for each subject separately, and both flexion ($r = 0.984 \pm 0.0144$) and extension ($r = 0.982 \pm 0.0165$). Although there are various joint torque estimation models [25], [26], this paper focuses on analyzing features of the results that appear when each signal is employed to recognize motion intention, and the above model is enough to recognize the intention in our tasks.

D. ANALYSIS OF RESULTS

To analyze the results from an agility perspective, we used the following metrics, considering the meaning of agility [27], [28]:

$$\text{agility} \propto \frac{1}{\int_{T_s}^{T_f} \mu_{raw}(t)dt} \cdot \frac{1}{\Delta T_e} \tag{7}$$

where T_s, T_f and ΔT_e denotes started time and finished time of the task; and elapsed time is represented by the difference between T_f and T_s which is $\Delta T_e = T_f - T_s$. $\int_{T_s}^{T_f} \mu_{raw}(t)dt$ denotes integrated sEMG (iEMG). The iEMG and elapsed time represent muscle effort and physical performance, respectively [4], [29].

In Experiment #1, we analyzed agility using only the iEMG values of the flexion muscle. This is because the task is restricted to the same motion ($\Delta T_e = 4.0$), and is slow enough not to use the extension muscle, as shown in Fig. 8. In Experiment #2, the agility is analyzed using iEMG of flexion muscle and elapsed time. This is because the task is for the flexion muscle, as shown in Fig. 9. The T_s is the start of reference, and T_f is the timing when the human limb position reaches the target position. In Experiment #3, the iEMG value of flexion and extension muscle and elapsed time were used to analyze the agility. The T_s and T_f are the start and end of the ten times of elbow motion.

The iEMG value and elapsed time were normalized based on the maximum values of each subject for each task [30], [31]. Additionally, the onset of each signal is detected by the threshold, which is set at (mean+3×standard deviation) measured before the start of each motion [32]. The pairwise comparisons were conducted for four conditions in three experiments.

The Kruskal–Wallis one-way analysis of variance test in Experiment #1 and permutation multivariate analysis of variance in Experiments #2 and #3 are performed [33], [34]. This is because the experiment's results did not follow normality according to the Shaprio-Wilk test, and Experiments #2 and #3 obtained results for interrelated multivariate variables, which are sEMG and task elapsed time. Statistical significance was set at a p-value < 0.05. All data comparisons were performed using MATLAB software (MATLAB 2020b Math; MathWorks Inc., MA, USA).

IV. RESULTS

In this section, we analyzed the results of the comparison experiments introduced in Section III-B from an agility perspective as explained in Section III-D.

A. EXPERIMENT #1: FOLLOWING REFERENCE TRAJECTORY

Fig. 8 shows the results of Experiment #1. The agility can be interpreted by comparing the iEMG value of flexion muscle as explained in Section III-D. For all the subjects, *sEMG-based* reduced the iEMG value of flexion compared to the *baseline*, while *F/T-based* reduced it only for the *no assistance* and not for the *baseline*. For the statistical analysis, there were significant differences in iEMG values of flexion muscle between *baseline* and *no assistance* ($p < .001$), *baseline* and *sEMG-based* ($p < .001$), *no assistance* and

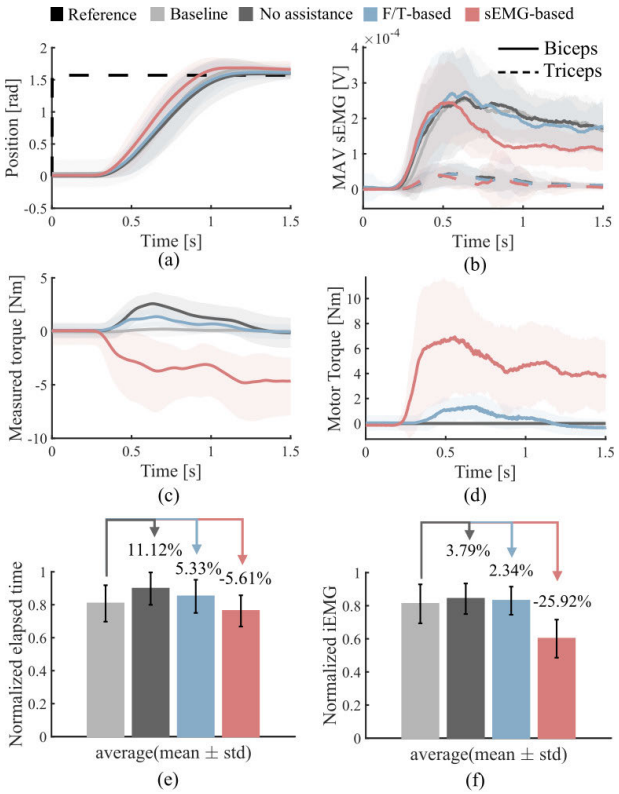

FIGURE 9. Experiment #2: Results for the step response experiment. (e) and (f) represents the total average and standard deviation of all subjects' results for the normalized elapsed time and iEMG value of flexion muscle, respectively. The percentage indicates the value compared to the *baseline* condition.

F/T-based ($p = .0055$), *no assistance* and *sEMG-based* ($p < .001$), and *F/T-based* and *sEMG-based* ($p < .001$), excluding between *baseline* and *F/T-based* ($p = .1463$).

B. EXPERIMENT #2: STEP RESPONSE

Fig. 9 shows the results of elapsed time and muscle usage to reach the target position, which is 90°. The agility can be interpreted by comparing the iEMG value of flexion muscle and elapsed time as explained in Section III-D. On average, *sEMG-based* reduced the iEMG value of the flexion muscle and elapsed time compared to the *baseline*. However, *F/T-based* reduced them only for the *no assistance* and not for the *baseline*. There were significant differences in agility between *baseline* and *no assistance* ($p < .001$), *baseline* and *sEMG-based* ($p < .001$), *no assistance* and *F/T-based* ($p = .03$), *no assistance* and *sEMG-based* ($p < .001$), and *F/T-based* and *sEMG-based* ($p < .001$), excluding between *baseline* and *F/T-based* ($p = .0581$).

Moreover, the time difference between the onset of the filtered sEMG signal and the F/T signal is approximately 100 ms, as the onset timing of the filtered sEMG signal is approximately 183 ms and the measured F/T signal is approximately 283 ms when the sEMG-based was used. It is also reflected in the timing of motor input, as shown in Fig.9-(d), because sEMG and F/T signal are command

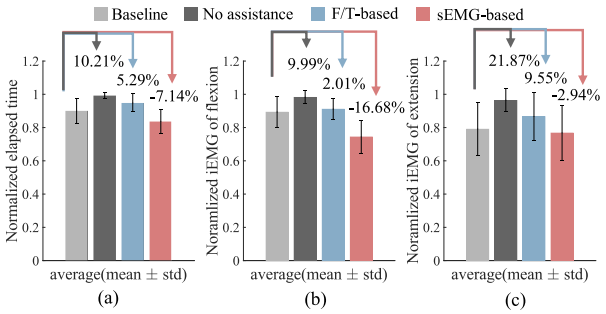

FIGURE 10. Experiment #3: Results of the maximum speed of repetitive movement experiment. (a), (b) and (c) show the elapsed time, and the iEMG value of flexion and extension muscles, respectively. The percentage indicates the value compared to the *baseline* condition.

sources of the *sEMG-based* and *F/T-based* control, respectively. This shows that the *sEMG-based* has more rapid assistance timing than the *F/T-based* control. As a result, the *sEMG-based* method can make rapid assistance and increase agility compared to *baseline* condition.

C. EXPERIMENT #3: MAXIMUM SPEED OF REPETITIVE MOVEMENT

Fig. 10 shows the experimental results for the Experiment #3. The agility can be interpreted by comparing the iEMG value of flexion and extension muscle and elapsed time, as explained in Section III-D. On average, *sEMG-based* reduced the iEMG values for flexion and extension muscles and elapsed time compared to the *baseline*. However, *F/T-based* control reduced them compared to the *no assistance* and not to the *baseline*. For the statistical analysis, there were significant differences in agility between *baseline* and *no assistance* ($p = .002$), *baseline* and *sEMG-based* ($p = .026$), *no assistance* and *F/T-based* ($p = .017$), *no assistance* and *sEMG-based* ($p < .001$), and *F/T-based* and *sEMG-based* ($p = .002$), excluding between *baseline* and *F/T-based* ($p = .2452$). As a result, the *sEMG-based* can enhance agility by reducing muscle usage and increasing the maximum speed.

V. DISCUSSION

According to the experimental results, agility increased when using the *sEMG-based* method compared to the *inherent motion* in the sense of muscle usage and elapsed time to take a task. On the other hand, the *F/T-based* method could enhance agility compared to the *no assistance* condition, whereas not for the *inherent motion*. This implies the *F/T-based* method can only reduce the impedance of the robot. In this section, further discussions take place about the experimental results and benefits of employing the sEMG signal to recognize human intention from an agility perspective. Also, the challenging issue of using sEMG signals is discussed.

A. BENEFITS OF SEMG SIGNAL: CORRECT RECOGNITION

We introduced the possibility of incorrect intention recognition by interaction F/T signal for increasing agility.

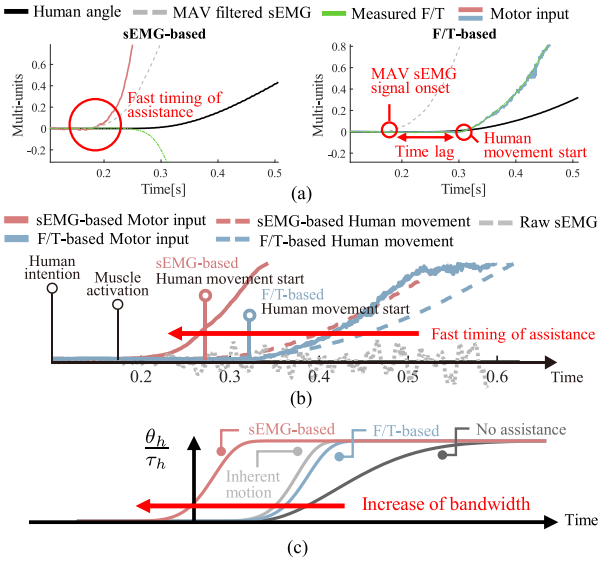

FIGURE 11. (a) Experimental results around the start of the motion from the step response experiment (Experiment #2). (b) Explanation of the rapid timing of assistance in the time domain with the procedure from human intention to movement. (c) Explanation of the step response results from the human input/output perspective for each condition.

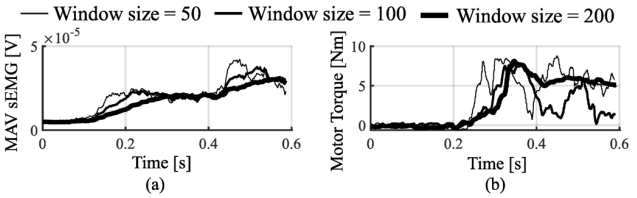

FIGURE 12. (a) MAV signal of same raw sEMG signal for three window sizes. (b) Motor input of *sEMG-based* control for three window sizes.

The experimental results can confirm this, as shown in Fig. 8-(c). When agility was enhanced via the *sEMG-based* method, the features of the F/T signal showed an extension (downward) direction both when the human body required robot assistance for the upward movement and when the forearm pushed the robot for extension movement. This implies that the interaction F/T signal has the same direction for different intentions. Additionally, when using the *F/T-based* method, the measured torque was approximately zero because the F/T signal was in the same direction as intention only when the human felt robot impedance. Therefore, the *F/T-based* method cannot enhance agility effectively compared to inherent body movement and only enhances agility compared to the *no assistance* condition while reducing the impedance of just the robot instead of the human-robot coupled system. In statistical analysis, the reason why *baseline* and *F/T-based* methods did not show a significant difference is also that the *F/T-based* method reduced the impedance of the robot, resulting in motions similar to *inherent motion*. As a result, the best scenario of the F/T-based method is to make the system equivalent to inherent movement since it can only reduce the robot's impedance. This provides experimental evidence that direct measurement is required for correct intention recognition to increase agility.

B. BENEFITS OF SEMG SIGNAL: RAPID ASSISTANCE TIMING

The results of Experiment #2 show that the *sEMG-based* method can react faster than the *F/T-based* method, implying that the *sEMG-based* method can reduce the time delay effect of the *F/T-based* method, as shown in Fig. 9-(d). Moreover, motor input can be applied before human motion initiation, as shown in Fig. 11-(a), via the *sEMG-based* method because it can be measured prior to human movement. Fig. 11 also shows that the IMU and F/T sensor have time-delayed issues.

As a result, we can expect an increase in bandwidth while reducing the response time via rapid assistance timing, as illustrated in Fig. 11-(c). Experiment #3 shows the possibility of an increase in the bandwidth of human movement since the maximum speed is increased through the rapid and correct assistance of *sEMG-based* control. Although in this study, we just used the fast timing of the sEMG signal, the optimal timing of assistance should be analyzed because it can affect the performance of assistance [35], [36]. Furthermore, since EMD varies depending on the muscle type and fatigue, it is important to consider these factors when adjusting assistance timing using the sEMG signal.

C. ATTENUATION EFFECT OF MAV FILTER

The MAV filter was used to deal with the noise of the sEMG signal. However, it could attenuate the current information of the signal according to the window size as it is the average value of the previous window size data. Fig. 12 shows the effect of the MAV filter based on window size. The same raw signal may also have different features, as shown in Fig. 12. As such, a trade-off between noise reduction and attenuation effect exists when using the sEMG signal. Therefore, the window size should be appropriately selected. It should be noted that the MAV signal contains current signal information because the new signal is not delayed by window size but attenuated by it.

D. MAGNITUDE OF MOTOR TORQUE

As observed in Fig 8-(d) and 9-(d), there is a difference in the magnitude of motor torque between F/T-based and sEMG-based methods. It is important to note that the presence (sEMG-based) or absence (F/T-based) of assistance is not determined by the magnitude of motor torque. The reason the motor torque could not be increased further in the F/T-based method is that reducing the robot's impedance through the F/T-based method allows the robot to better adjust to and follow human movements, resulting in lower interaction forces. These reduced interaction forces, in turn, limit the magnitude of the control input in F/T-based control. Suppose the robot's impedance is decreased and the gain is increased to enhance motor torque in the F/T-based method. In that case,

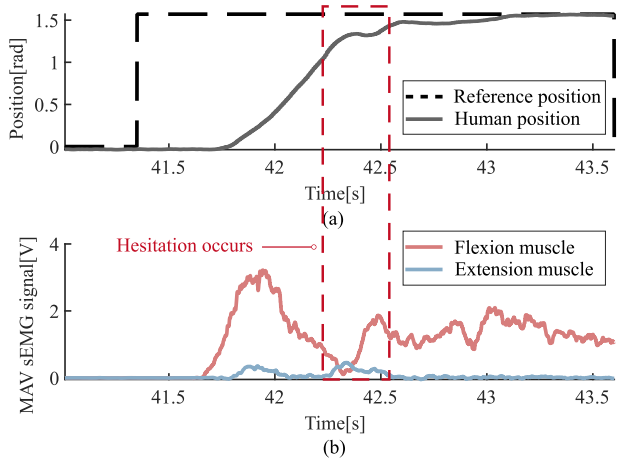

FIGURE 13. An example of hesitation during the step response task (Experiment #2). (a) Human limb position (b) MAV sEMG signal of flexion and extension muscle. The subject hesitates to move the limb and uses the flexion muscle, which is used to lift the limb (flexion motion), but uses the extension muscle to resist the motion.

the robot may oscillate because the F/T-based method fails to recognize human intention correctly, leading to a repetition of the situations described in Fig 3-(a) and 3-(b), causing the robot to oscillate. The results from three experiments showing that the F/T-based method has lower agility compared to inherent motion also demonstrate that the magnitude of motor input does not determine the presence of assistance.

There was also a psychological effect for the magnitude of motor torque. In particular, when using the sEMG-based method, there were cases where the robot's assistance was awkward or was afraid of being too high of assistance. This is because most people have rarely experienced being assisted at a fast timing and move at a faster speed than the maximum speed of inherent body movement. As a result, a situation of hesitation occurs while taking the step response task, such as Fig. 13.

VI. CONCLUSION

This study discussed the benefits of employing sEMG signals for power-assisted control to recognize the intention from an agility perspective. Therefore, we conducted three comparison experiments with four conditions, which are *inherent motion*, *no assistance*, *F/T-based*, and *sEMG-based*. The experimental results demonstrate that the *sEMG-based* method enhanced agility compared to inherent body movement, while the *F/T-based* method only reduced the robot's impedance. The *sEMG-based* method reduced flexion muscle usage by 29.45% in the following trajectory task, reduced flexion muscle usage by 25.92% and elapsed time by 5.61% in the step response task, and reduced flexion muscle usage by 16.68% and elapsed time by 7.14% in the maximum speed of repetitive movement task, compared to inherent body movement. As a result, we confirmed that sEMG-based control could enhance agility through rapid and direct measurement of motion intention while addressing the limitations of the F/T signal for agile movement. These results can offer guidance on selecting the appropriate signal for recognizing motion intention with the characteristics of each signal.

Our study is limited to healthy male subjects and focuses on simple elbow motion. Therefore, based on the benefits of employing sEMG signals for power-assisted control from the agility perspective we analyzed in this study, we plan to expand the results for diverse participants and motions in future works. Furthermore, we plan to progress towards power-assisted control by merging the advantages of F/T signals and sEMG signals. We will also consider the assistance timing and other direct signals, such as brain signals, as future works.

ACKNOWLEDGMENT

The authors would like to express their gratitude to all the volunteers who participated in this study. They also thank Yeoeun Kim in POSTECH for the support in improving the figures in this paper.

REFERENCES

[1] S. Jacobsen, "On the development of XOS, a powerful exoskeletal robot," in *Proc. IEEE/RSJ Int. Conf. Intell. Robots Syst.*, Aug. 2007, pp. 1–12.
[2] E. Helms, R. D. Schraft, and M. Hagele, "Rob@work: Robot assistant in industrial environments," in *Proc. 11th IEEE Int. Workshop Robot Hum. Interact. Commun.*, Oct. 2002, pp. 399–404.
[3] D. Aoyagi, W. E. Ichinose, S. J. Harkema, D. J. Reinkensmeyer, and J. E. Bobrow, "A robot and control algorithm that can synchronously assist in naturalistic motion during body-weight-supported gait training following neurologic injury," *IEEE Trans. Neural Syst. Rehabil. Eng.*, vol. 15, no. 3, pp. 387–400, Sep. 2007.
[4] J. M. Sheppard and W. B. Young, "Agility literature review: Classifications, training and testing," *J. Sports Sci.*, vol. 24, no. 9, pp. 919–932, Sep. 2006.
[5] Q. Ma, L. Ji, and R. Wang, "The development and preliminary test of a powered alternately walking exoskeleton with the wheeled foot for paraplegic patients," *IEEE Trans. Neural Syst. Rehabil. Eng.*, vol. 26, no. 2, pp. 451–459, Feb. 2018.
[6] V. Maheu, P. S. Archambault, J. Frappier, and F. Routhier, "Evaluation of the JACO robotic ARM: Clinico-economic study for powered wheelchair users with upper-extremity disabilities," in *Proc. IEEE Int. Conf. Rehabil. Robot.*, Jun. 2011, pp. 1–5.
[7] W. Huo, S. Mohammed, Y. Amirat, and K. Kong, "Fast gait mode detection and assistive torque control of an exoskeletal robotic orthosis for walking assistance," *IEEE Trans. Robot.*, vol. 34, no. 4, pp. 1035–1052, Aug. 2018.
[8] Z. Li, B. Huang, Z. Ye, M. Deng, and C. Yang, "Physical human–robot interaction of a robotic exoskeleton by admittance control," *IEEE Trans. Ind. Electron.*, vol. 65, no. 12, pp. 9614–9624, Dec. 2018.
[9] J. Huang, W. Huo, W. Xu, S. Mohammed, and Y. Amirat, "Control of upper-limb power-assist exoskeleton using a human–robot interface based on motion intention recognition," *IEEE Trans. Autom. Sci. Eng.*, vol. 12, no. 4, pp. 1257–1270, Oct. 2015.
[10] M. J. Kim, W. Lee, J. Y. Choi, G. Chung, K.-L. Han, I. S. Choi, C. Ott, and W. K. Chung, "A passivity-based nonlinear admittance control with application to powered upper-limb control under unknown environmental interactions," *IEEE/ASME Trans. Mechatronics*, vol. 24, no. 4, pp. 1473–1484, Aug. 2019.
[11] S. R. Soekadar, M. Witkowski, C. Gómez, E. Opisso, J. Medina, M. Cortese, M. Cempini, M. C. Carrozza, L. G. Cohen, N. Birbaumer, and N. Vitiello, "Hybrid EEG/EOG-based brain/neural hand exoskeleton restores fully independent daily living activities after quadriplegia," *Sci. Robot.*, vol. 1, no. 1, Dec. 2016, Art. no. eaag3296.
[12] T. Lenzi, S. M. M. De Rossi, N. Vitiello, and M. C. Carrozza, "Intention-based EMG control for powered exoskeletons," *IEEE Trans. Biomed. Eng.*, vol. 59, no. 8, pp. 2180–2190, Aug. 2012.

[13] Y. Zhuang, Y. Leng, J. Zhou, R. Song, L. Li, and S. W. Su, "Voluntary control of an ankle joint exoskeleton by able-bodied individuals and stroke survivors using EMG-based admittance control scheme," *IEEE Trans. Biomed. Eng.*, vol. 68, no. 2, pp. 695–705, Feb. 2021.
[14] R. J. Downey, M. Merad, E. J. Gonzalez, and W. E. Dixon, "The time-varying nature of electromechanical delay and muscle control effectiveness in response to stimulation-induced fatigue," *IEEE Trans. Neural Syst. Rehabil. Eng.*, vol. 25, no. 9, pp. 1397–1408, Sep. 2017.
[15] J. Lee, M. Kim, and K. Kim, "A control scheme to minimize muscle energy for power assistant robotic systems under unknown external perturbation," *IEEE Trans. Neural Syst. Rehabil. Eng.*, vol. 25, no. 12, pp. 2313–2327, Dec. 2017.
[16] N. Lotti, M. Xiloyannis, F. Missiroli, C. Bokranz, D. Chiaradia, A. Frisoli, R. Riener, and L. Masia, "Myoelectric or force control? A comparative study on a soft arm exosuit," *IEEE Trans. Robot.*, vol. 38, no. 3, pp. 1363–1379, Jun. 2022.
[17] A. C. Villa-Parra, D. Delisle-Rodriguez, T. Botelho, J. J. V. Mayor, A. L. Delis, R. Carelli, A. Frizera Neto, and T. F. Bastos, "Control of a robotic knee exoskeleton for assistance and rehabilitation based on motion intention from sEMG," *Res. Biomed. Eng.*, vol. 34, no. 3, pp. 198–210, Jul. 2018.
[18] D. Ao, R. Song, and J. Gao, "Movement performance of human–robot cooperation control based on EMG-driven hill-type and proportional models for an ankle power-assist exoskeleton robot," *IEEE Trans. Neural Syst. Rehabil. Eng.*, vol. 25, no. 8, pp. 1125–1134, Aug. 2017.
[19] D. Novak and R. Riener, "A survey of sensor fusion methods in wearable robotics," *Robot. Auto. Syst.*, vol. 73, pp. 155–170, Nov. 2015.
[20] S. Kyeong, W. Shin, M. Yang, U. Heo, J.-R. Feng, and J. Kim, "Recognition of walking environments and gait period by surface electromyography," *Frontiers Inf. Technol. Electron. Eng.*, vol. 20, no. 3, pp. 342–352, Mar. 2019.
[21] R. M. Murray, Z. Li, and S. S. Sastry, *A Mathematical Introduction to Robotic Manipulation*. Boca Raton, FL, USA: CRC Press, 2017.
[22] H. J. Hermens, B. Freriks, R. Merletti, D. Stegeman, J. Blok, G. Rau, C. Disselhorst-Klug, and G. Hägg, "European recommendations for surface electromyography," *Roessingh Res. Dev.*, vol. 8, no. 2, pp. 13–54, 1999.
[23] K. Kiguchi, T. Tanaka, and T. Fukuda, "Neuro-fuzzy control of a robotic exoskeleton with EMG signals," *IEEE Trans. Fuzzy Syst.*, vol. 12, no. 4, pp. 481–490, Aug. 2004.
[24] K. Ullah and J.-H. Kim, "A mathematical model for mapping EMG signal to joint torque for the human elbow joint using nonlinear regression," in *Proc. 4th Int. Conf. Auto. Robots Agents*, Feb. 2009, pp. 103–108.
[25] E. Ceseracciu, A. Mantoan, M. Bassa, J. C. Moreno, J. L. Pons, G. A. Prieto, A. J. del Ama, E. Marquez-Sanchez, Á. Gil-Agudo, C. Pizzolato, D. G. Lloyd, and M. Reggiani, "A flexible architecture to enhance wearable robots: Integration of EMG-informed models," in *Proc. IEEE/RSJ Int. Conf. Intell. Robots Syst. (IROS)*, Sep. 2015, pp. 4368–4374.
[26] T. Teramae, T. Noda, and J. Morimoto, "EMG-based model predictive control for physical human–robot interaction: Application for assist-as-needed control," *IEEE Robot. Autom. Lett.*, vol. 3, no. 1, pp. 210–217, Jan. 2018.
[27] T. Zhang, M. Tran, and H. Huang, "Admittance shaping-based assistive control of SEA-driven robotic hip exoskeleton," *IEEE/ASME Trans. Mechatronics*, vol. 24, no. 4, pp. 1508–1519, Aug. 2019.
[28] J. Arnold, H. Hanzlick, and H. Lee, "Variable damping control of the robotic ankle joint to improve trade-off between performance and stability," in *Proc. Int. Conf. Robot. Autom. (ICRA)*, May 2019, pp. 1699–1704.
[29] J. H. T. Viitasalo and P. V. Komi, "Signal characteristics of EMG during fatigue," *Eur. J. Appl. Physiol. Occupational Physiol.*, vol. 37, no. 2, pp. 111–121, 1977.
[30] M. Halaki and K. Ginn, "Normalization of EMG signals: To normalize or not to normalize and what to normalize to," *Comput. Intell. Electromyogr. Analysis—A perspective Current Appl. Future Challenges*, vol. 10, p. 49957, Aug. 2012.
[31] W. R. Nicholson, "The importance of normalization in the interpretation of surface electromyography: A proof of principle," *J. Manipulative Physiological Therapeutics*, vol. 23, no. 5, pp. 0369–0370, Jun. 2000.
[32] C. R. Carvalho, J. M. Fernández, A. J. Del-Ama, F. O. Barroso, and J. C. Moreno, "Review of electromyography onset detection methods for real-time control of robotic exoskeletons," *J. NeuroEngineering Rehabil.*, vol. 20, no. 1, p. 141, Oct. 2023.
[33] M. J. Anderson, "A new method for non-parametric multivariate analysis of variance," *Austral Ecology*, vol. 26, no. 1, pp. 32–46, Jun. 2008.
[34] W. C. Navidi, *Statistics for Engineers and Scientists*, vol. 2. New York, NY, USA: McGraw-Hill, 2006.
[35] I. Kang, H. Hsu, and A. Young, "The effect of hip assistance levels on human energetic cost using robotic hip exoskeletons," *IEEE Robot. Autom. Lett.*, vol. 4, no. 2, pp. 430–437, Apr. 2019.
[36] A. J. Young, J. Foss, H. Gannon, and D. P. Ferris, "Influence of power delivery timing on the energetics and biomechanics of humans wearing a hip exoskeleton," *Frontiers Bioengineering Biotechnol.*, vol. 5, p. 4, Mar. 2017.

JAEWON BYUN received the B.S. and M.S. degrees in mechanical engineering from Pohang University of Science and Technology, Pohang, South Korea, in 2017 and 2022, respectively, where he is currently pursuing the Ph.D. degree in mechanical engineering.

KEEHOON KIM (Senior Member, IEEE) received the B.S., M.S., and Ph.D. degrees in mechanical engineering from Pohang University of Science and Technology, Pohang, South Korea, in 1999, 2001, and 2006, respectively. He was a Visiting Student with Case Western Reserve University, Cleveland, OH, USA, from 2003 to 2004. He was a Postdoctoral Researcher with the Department of Mechanical Engineering, Northwestern University, Evanston, IL, USA, from 2006 to 2009. From 2009 to 2015, he was a Senior Research Scientist with Korea Institute of Science and Technology, where he was a Principal Research Scientist, from 2015 to 2019. From 2018 to 2019, he was a Visiting Professor with the Mechanical Engineering Department, The University of Texas at Austin. Since 2019, he has been an Associate Professor with Pohang University of Science and Technology. His research interests include robotics in biomedical applications, including rehabilitation robotics, surgical robotics, power assistant robotics and bionics, haptic interfaces, and teleoperation. Since 2016, he has been serving as the Co-Chair for the IEEE RAS Technical Committee of Telerobotics. From 2015 to 2018, he served as an Editor for the IEEE/RSJ International Conference on Intelligent Robots and Systems. Since 2024, he has been serving as an Associate Editor for IEEE Robotics and Automation Letters.